General Disclaimer

One or more of the Following Statements may affect this Document

- This document has been reproduced from the best copy furnished by the organizational source. It is being released in the interest of making available as much information as possible.

- This document may contain data, which exceeds the sheet parameters. It was furnished in this condition by the organizational source and is the best copy available.

- This document may contain tone-on-tone or color graphs, charts and/or pictures, which have been reproduced in black and white.

- This document is paginated as submitted by the original source.

- Portions of this document are not fully legible due to the historical nature of some of the material. However, it is the best reproduction available from the original submission.

NASA TECHNICAL MEMORANDUM

NASA TM X-73550

NASA TM X-73550

10^0 OFF-AXIS TEST FOR SHEAR PROPERTIES IN FIBER COMPOSITES

by C. C. Chamis and J. H. Sinclair
Lewis Research Center
Cleveland, Ohio 44135

TECHNICAL PAPER to be presented at the
Spring Meeting of the Society for
Experimental Stress Analysis
Dallas, Texas, May 15-20, 1977

10° OFF-AXIS TEST FOR SHEAR PROPERTIES IN FIBER COMPOSITES

It is demonstrated that the 10° off-axis tensile test is an accurate and convenient test method for the intralaminar shear characterization of unidirectional fiber composites.

by C. C. Chamis* and J. H. Sinclair*

National Aeronautics and Space Administration
Lewis Research Center
Cleveland, Ohio 44135

ABSTRACT

A combined theoretical and experimental investigation was conducted to assess the suitability of the 10° off-axis tensile test specimen for the intralaminar shear characterization of unidirectional composites. Composite mechanics, a combined-stress failure criterion, and a finite element analysis were used to determine theoretically the stress-strain variation across the specimen width and the relative stress and strain magnitudes at the 10° plane. Strain gages were used to measure the strain variation across the specimen width at specimen midlength and near the end tabs. Specimens from Mod-I/epoxy, T-300/epoxy, and S-glass/epoxy were used in the experimental program. It was found that the 10° off-axis tensile test specimen is suitable for intralaminar shear characterization and it is recommended that it should be considered as a possible standard test specimen for such a characterization.

---

*Aerospace structures research engineers, Composites Branch, NASA Lewis Research Center.

LIST OF SYMBOLS

E	normal modulus; subscripts define direction
F	combined-stress failure criterion function
G	shear modulus-intralaminar
K	coupling coefficient in combined-stress failure criterion function
S	uniaxial fracture stress; subscripts define direction
x,y,z	structural-axes orthogonal coordinate system with x taken along load direction
$1,2,3$	material-axes orthogonal coordinate system with 1 taken along fiber direction
ε	strain; subscripts define type, plane, and direction
θ	orientation angle between structural and material axes measured positive counterclockwise
θ_g	orientation angle locating strain gage from load direction
σ	stress; subscripts define type, plane, and direction

Subscripts:

C	compression
c	structural axes property
g	strain gage reading
ℓ	ply (unidirectional composite) property
S	shear, symmetric
T	tension
x,y,z	structural axes directions
$1,2,3$	material axes directions

INTRODUCTION

Efficient intralaminar (in-plane) shear characterization of unidirectional fiber composites has been a problem because of the difficulty of producing a state of pure shear in practical laboratory test specimens. For example, the simplest test specimen in use today is the three-point-bend short-beam-shear test specimen (ASTM D-2344-72). But this test specimen, while expedient for material quality control, is not suitable for generating design data because (1) this test produces nonuniform shear stress through the specimen's thickness and (2) the test yields only the fracture stress and not the total shear-stress shear-strain record to fracture. The most desirable test specimen is the thin tube subjected to torsion. This specimen provides pure shear stress and strain in the wall of the tube; however, the tube specimen is too expensive and time consuming to be practical and efficient. Between these two extremes, several other test specimens and procedures have been proposed for intralaminar shear characterization of unidirectional fiber composites.[1] None of the available test specimens is completely satisfactory and researchers in the field are continuously looking for and proposing new ones.

One recent test specimen is the 10° off-axis tensile specimen proposed by IIT Research Institute during the course of an investigation under contract to NASA Lewis Research Center.[2] This test specimen has several desirable features to qualify it as an efficient and a possible standard test for intralaminar shear characterization. However, it was recognized that before considering it as a possible standard, additional investigation was required from both the theoretical and experimental

viewpoints.

Therefore, the objectives of the investigation reported herein were to perform both detailed theoretical and experimental studies in order to assess the suitability of the 10° off-axis tensile specimen for intralaminar shear characterization and the possibility for recommending it as a standard test specimen for such a characterization.

THEORY

Relative Stress Magnitudes at the 10° Plane from Force Equilibrium

A biaxial stress state is present when a 10° off-axis specimen is subjected to a uniaxial load. As is indicated in Fig. 1, this biaxial stress state consists of three stresses, longitudinal $\sigma_{\ell 11}$, transverse $\sigma_{\ell 22}$, and intralaminar shear $\sigma_{\ell 12}$ at the 10° plane. If a 10° off-axis specimen is to serve as a means for intralaminar shear characterization of a uniaxial composite, the intralaminar shear stress $\sigma_{\ell 12}$ must be the only one of these three stresses that is near its critical value, and fracture must occur at the 10° plane when $\sigma_{\ell 12}$ reaches this critical value.

The stresses in a ply with fibers oriented at an angle θ from the load direction as a function of the applied stress σ_{cxx} are given by the following well known transformation equations which are easily derivable from force equilibrium considerations:

$$\sigma_{\ell 11} = \sigma_{cxx} \cos^2\theta \tag{1}$$

$$\sigma_{\ell 22} = \sigma_{cxx} \sin^2\theta \tag{2}$$

$$\sigma_{\ell 12} = \frac{1}{2} \sigma_{cxx} \sin 2\theta \tag{3}$$

The notation in Eqs. (1) to (3) is as follows: σ denotes stress; θ is the orientation angle between applied stress (load direction) and the fiber direction; the subscripts c and ℓ denote composite and ply, respectively; the numerical subscripts 1 and 2 refer to an orthogonal right-hand coordinate system with 1 taken along the fiber direction. For the 10° off-axis specimen, substituting 10° for θ in Eqs. (1) to (3) yields the following to three decimal figures:

$$\sigma_{\ell 11} = 0.970\ \sigma_{cxx} \tag{4}$$

$$\sigma_{\ell 22} = 0.030\ \sigma_{cxx} \tag{5}$$

$$\sigma_{\ell 12} = 0.171\ \sigma_{cxx} \tag{6}$$

Eqs. (5) and (6) are used to assess the relative magnitudes of the transverse and intralaminar shear stresses. As can be seen from Eqs. (5) and (6), the intralaminar shear stress is about six times greater than the transverse stress.

Data comparing the relative magnitudes of the fracture strengths for a high modulus graphite epoxy system are presented in table I. In table I(a), under "Load direction," four types of specimens are listed. The first, second, and fourth were tensile specimens prepared from an eight-ply, flat, uniaxial $[0]_8$ laminate of Mod-I/epoxy (ERLA 4617). The specimens were cut out of the laminate so that the tensile axis of the 0° specimen was parallel to the fiber direction of the laminate, that of the 90° specimen was perpendicular to the fiber direction, and the tensile axis of the 10° specimen was offset 10° from the fiber direction of the laminate. The third specimen shown in table I(a) was a 5.08-centimeter-

(2-in.) diameter eight-ply Mod-I/epoxy tube with the graphite fibers running lengthwise along the tube. This tube was tested in torsion.

The fracture strength σ_{cxx} of the 10° off-axis composite (item 4, table I(a)) was 34.3×10^{3} N/cm^2 (49.8 ksi). The corresponding fracture stresses of the plies at the 10° plane ($\sigma_{\ell 11}$, $\sigma_{\ell 22}$, and $\sigma_{\ell 12}$) as computed using Eqs. (4) to (6) are presented in table I(b). The ratios of the computed ply fracture stresses to the measured uniaxial fracture strengths are shown in table I(c). As can be seen in table I(c), only the computed intralaminar shear stress is near its critical value.

Relative Stress Magnitudes from Combined-Stress Failure Criteria

In the previous section the relative stress magnitudes were compared on an individual stress basis and combined-stress interaction is not taken into account. To account for the interaction, a combined-stress failure criterion is required. The combined-stress failure criterion used herein is derivable from a modified distortion energy principle which is described in Refs. 3 and 4. When both the ply longitudinal and the transverse stresses are tensile, as is the case for the 10° off-axis tensile specimen, the failure criterion to determine whether fracture has occurred is

$$1 - \left[\left(\frac{\sigma_{\ell 11}}{S_{\ell 11T}}\right)^2 + \left(\frac{\sigma_{\ell 22}}{S_{\ell 22T}}\right)^2 - K_{\ell 12}\,\frac{\sigma_{\ell 11}\sigma_{\ell 22}}{S_{\ell 11T}S_{\ell 22T}} + \left(\frac{\sigma_{\ell 12}}{S_{\ell 12S}}\right)^2\right] \leq 0 \qquad (7)$$

where S denotes uniaxial fracture stress, K is a coupling coefficient which depends on the elastic constants of the composite material,[3 or 4] the subscript T denotes tension and S denotes shear. Using numerical values for σ and S from table I(a) and the corresponding K value of

1.44 as determined in Refs. 3 and 4, Eq. (7) yields

$$1 - [0.350 + 0.141 - 0.319 + 1.25] = -0.421$$

Since this value is less than zero, according to the failure criterion, fracture has occurred. The important observation to be noted here is that the major stress contribution to fracture is from the intralaminar shear stress which is the last term in the brackets. The contribution from the longitudinal and transverse stresses (first three terms in the brackets) tend to cancel each other.

Sensitivity of Material-Axis Stresses and Strains with Errors in Orientation Angle

An assessment of how sensitive the material-axes stresses and strains are with small errors in the load orientation angle may be obtained by plotting these stresses against orientation angle. This is illustrated in Fig. 2, where the ply stresses plotted have been normalized with respect to composite stress along the load direction. The important point to be observed from this figure is that in the region of a load angle of 10°, the transverse and intralaminar shear stresses vary more rapidly than the longitudinal stress on a relative basis. It can be shown that a 1° change (e.g., $\theta = 11^{\circ}$ in Eqs. (1) to (3)) in load angle produces a change of about 21 percent in the transverse stress, a 10-percent change in the intralaminar shear stress, and only a 0.6-percent change in the longitudinal stress.

The variation of the material-axes strains as a function of load angle is plotted in Fig. 3 for a Mod-I/epoxy unidirectional composite. As can be observed in this figure, the material-axes shear strain (intralaminar shear strain $\varepsilon_{\ell 12}$) is maximum at about a 10° load orientation

angle and appears to be insensitive to small errors about this angle. These are significant results because they are desirable features for the test specimen proposed to measure the intralaminar shear modulus and fracture shear stress. Though results are not presented here, the two other composites investigated approach their peaks at about 11° for T-300/epoxy (PR288) and 15° for S-glass/epoxy (PR288).

The previous discussion leads to the following conclusion. Since ply intralaminar shear stress of the 10° off-axis tensile specimen is sensitive to small misorientation errors, care should be taken in fiber orientation, strain gage positioning, and load alinement. It is recommended that these be kept within $\pm 1^{\circ}$. However, if the fracture intralaminar shear strain is sought, then the misorientation is not as critical since the intralaminar shear strain peaks at load angle of about 10° and is insensitive to small errors about this angle.

Equations for Generating the Ply Intralaminar Shear Stress-Strain Curve

The well known equation relating the ply intralaminar shear strain to structural-axes strain for any θ orientation is

$$\varepsilon_{\ell 12} = (\varepsilon_{cyy} - \varepsilon_{cxx})\sin 2\theta + \varepsilon_{cxy} \cos 2\theta \tag{8}$$

The structural axes strains $\{\varepsilon_c\}$ for a 60°-delta rosette ($\theta_{g1} = 0^{\circ}$; $\theta_{g2} = 120^{\circ}$; $\theta_{g3} = 240^{\circ}$, Fig. 4) are given by

$$\left.\begin{aligned} \varepsilon_{cxx} &= \varepsilon_{g1} \\ \varepsilon_{cyy} &= \frac{2\varepsilon_{g2} + 2\varepsilon_{g3} - \varepsilon_{g1}}{3} \\ \varepsilon_{cxy} &= \frac{2(\varepsilon_{g3} - \varepsilon_{g2})}{\sqrt{3}} \end{aligned}\right\} \tag{9}$$

The intralaminar shear strain along the 10° plane is obtained by substituting the structural-axis strains from Eq. (9) in Eq. (8) and setting $\theta = 10^{\circ}$. The resulting equation in three decimal figures is

$$\varepsilon_{\ell 12} = -0.456\ \varepsilon_{g1} - 0.857\ \varepsilon_{g2} + 1.313\ \varepsilon_{g3} \tag{10}$$

The structural axes strains for a rectangular rosette ($\theta_{g1} = 0^{\circ}$; $\theta_{g2} = 45^{\circ}$; and $\theta_{g3} = 90^{\circ}$, Fig. 4) are given by

$$\left.\begin{aligned} \varepsilon_{cxx} &= \varepsilon_{g1} \\ \varepsilon_{cyy} &= \varepsilon_{g3} \\ \varepsilon_{cxy} &= -\varepsilon_{g1} + 2\varepsilon_{g2} - \varepsilon_{g3} \end{aligned}\right\} \tag{11}$$

The intralaminar shear strain along the 10° plane is obtained in the same way as described for the 60°-delta rosette. The resulting equation is

$$\varepsilon_{\ell 12} = -1.282\ \varepsilon_{g1} + 1.879\ \varepsilon_{g2} - 0.598\ \varepsilon_{g3} \tag{12}$$

As can be seen from Eqs. (10) and (12) the calculation for the intralaminar shear strain is simple once the true gage strains are known. The strains ε_{g1}, ε_{g2}, and ε_{g3} are the true gage strains in that they account for gage transverse sensitivity provided by the gage manufacturer.[5]

The procedure for generating the intralaminar shear stress-strain curve is as follows: For each load increment,

(1) Calculate the intralaminar shear strain from either Eq. (10) for a 60°-delta rosette or from Eq. (12) for a rectangular rosette.

(2) Calculate the ply intralaminar shear stress $\sigma_{\ell 12}$ from Eq. (6).

(3) Plot $\sigma_{\ell 12}$ calculated in item (2) against $\varepsilon_{\ell 12}$ calculated in item (1).

The initial ply shear modulus is determined from the slope of the initial

tangent to the stress-strain curve plotted in item (3). The shear modulus at any other point may be determined from the slope of the tangent to the curve at that point. The ply intralaminar shear strength equals the shear stress calculated in item (2) at the fracture load. The ply intralaminar fracture strain is the shear strain calculated at the fracture load in item (1).

It is important to note that the generation of the intralaminar shear stress-strain curve from the procedure just described requires the simultaneous readings of three strain gages and the relatively simple calculations already indicated.

Axial Stress Variation Across the Specimen Width at Midlength Via Finite Element Analysis

In order to obtain a theoretical assessment of the axial stress variation due to in-plane bending induced by the end tabs, a finite element analysis was performed. The element used is a second-order triangular plate finite element with six nodes and two displacement degrees of freedom (DOF) per node. A schematic of the finite element representation is shown in Fig. 5. The dimensions shown in the schematic are those of the actual test specimen used. Note the finite element representation includes the tapered end-tab portions, and consists of 288 elements, 657 nodes, and 1314 DOF.

The analysis was performed on a specimen made from Mod-I/epoxy and having three different boundary conditions. The boundaries were selected to simulate the following:

(1) Fixed ends, induces in-plane bending

(2) Pinned ends, free from in-plane bending

(3) End load equivalent to produce an end restraint intermediate to (1) and (2)

The finite element analysis results are presented graphically in Fig. 6 . The actual boundary conditions of the specimen produce a stress variation somewhere between (1) and (2) and probably close to (3). The important points to be observed from the curves in Fig. 6 are:

(1) At the specimen center all boundary conditions induce approximately the same axial stress which is equal to the average stress P/A in the specimen.

(2) The axial stress variation across the specimen width will be less than 10 percent assuming the dash-dotted curve is the best approximation.

(3) The axial stress at one edge may be 2 to 5 percent higher than the axial stress at the center. This observation has the following significant implication. Because the edge stress is higher, fracture will probably initiate at the edge. The average axial stress as predicted by P/A will be a few percent less than the axial stress at the edge which initiates fracture. Therefore, the intralaminar fracture stress predicted by Eq. (6) is on the conservative side.

EXPERIMENTAL INVESTIGATION

Composite Systems

The composite systems used in this investigation consisted of 8-ply Mod-I/ERLA 4617-epoxy, T-300/PR 288-epoxy, and S-glass/PR 288-epoxy. These were selected in order to determine the applicability of the test

specimen at high, intermediate, and low orthotropicity (longitudinal modulus to transverse modulus $E_{\ell 11}/E_{\ell 22}$) ratios, respectively. The Mod-I/epoxy laminate was supplied by a commercial vendor. The other two were fabricated in-house from commercially available prepreg and according to vendor's fabrication procedure. Measured unidirectional mechanical properties of these laminates are summarized in table II.

Specimen Preparation, Instrumentation, and Testing

A drafting machine was used to lay out tensile specimens at 10^{c} load angles on the laminate plates. The specimens were then cut slightly overwidth by a 0.061-centimeter- (0.024-in.) thick diamond wheel mounted on a surface grinder. Stacks of specimens, so cut, were placed on edge and dressed down to the required 1.27-centimeter (0.500-in.) width by a diamond wheel. Specimen ends were reinforced with adhesively bonded fiberglass tabs.

Tensile specimens were instrumented with either one (at center) or five (three at center, two near ends) strain gages, type EA-13-030YB-120, 60^{o} delta rosette. The test specimens were placed in the test fixture and loaded to fracture using a hydraulically actuated universal testing machine. Loading was incremental to facilitate periodic recording of strain gage data.

Axial Strain Variations Across Specimen Widths

Axial strains at fracture are shown in Fig. 7 for Mod-I/epoxy. These data taken directly from the stress-strain data are accompanied on the figure with a schematic of the specimen and plots of strain against gage location.

The experimentally measured fracture strains are slightly higher at the specimen edges than at the center (0.320 and 0.336 percent compared to 0.287 percent) for the gages located at the midlength. Near the tensile grips, however, the strain was higher halfway across the specimen (0.305 percent) than near the edge (0.288 percent). It is suspected that these differences are due primarily to the restraining effects of the grips. The important point to observe is that the difference between the axial strains at the edges (at the specimen midlength) is less than 5 percent.

Shear Stress-Strain Curves

Intralaminar shear stress-strain curves of the 10° off-axis tensile specimen for Mod-I/epoxy, S-glass/epoxy, and T-300/epoxy are presented in Fig. 8. The intralaminar shear stresses and shear strains were calculated from data obtained from the SGDR[6] program (table III) by using Eqs. (6) and (8). Note Eq. (10) could also have been used. The intralaminar shear stresses $\sigma_{\ell 12}$ thus obtained were plotted against the intralaminar shear strains $\epsilon_{\ell 12}$ calculated for the corresponding longitudinal tensile stresses.

Observations of the intralaminar shear stress-strain diagrams (Fig. 8) reveal that initially the S-glass composite is most resistant to shear deformation followed by the Mod-I and T-300 in that orde . At failure, however, Mod-I is more resistant to shear with S-glass having the least shear resistance. Note the extensive nonlinearity of the diagrams for the S-glass and T-300 curves.

A photograph of the Mod-I fractured specimen is shown in Fig. 9. As

can be seen in this figure, the fracture occurred at the gage section along the fiber direction indicating intralaminar shear fracture.

Comparisons of Mod-I/Epoxy Shear Stress-Strain Curves for Different Configurations and Layups

Shear stress-strain curves for some additional Mod-I/epoxy laminate configurations along with the curve for $[0]_8$ tested at 10° from the fiber direction (10° off-axis tensile specimen) are shown in Fig. 10 for comparison purposes. The additional curves are for a $[0_2,90_2]_S$ laminate tested at 10° to the 0° fiber direction, a $\pm 45^\circ$ laminate, and for a unidirectional thin tube tested in torsion in the Lewis Research Center Multiaxial Testing Facility.[7] Note that the initial tangents are approximately the same for all four laminate configurations. However, as can be observed from Fig. 10, the fracture shear strains of the 10° off-axis tensile specimen and the thin tube are about the same. Those for the other two are about 30-percent lower. This lower value reflects the presence of transverse lamination residual stress in the $[0_2,90_2]_S$ (tested at 10°) and the $[(\pm 45)_2]_S$ laminates.

The important observation from the previous discussion is that the 10° off-axis tensile specimen had an intralaminar fracture shear strain practically identical to that of the thin tube tested in torsion and a corresponding stress about 0.66×10^3 N/cm^2 (1 ksi) higher. Therefore, the 10° off-axis tensile specimen should be suitable for intralaminar shear characterization.

COMPARISONS

The measured and finite element predicted structural axes shear strains are plotted in Fig. 11 for the same axial stress for comparison

purposes. As can be seen, the comparison is reasonable. It is noted that this comparison was selected because of the predominance of the structural axes shear strains relative to the other two strains (Fig. 3).

The measured-initial-tangent intralaminar shear moduli and fracture stresses are compared with those available elsewhere (low and high values) in table III. As can be seen, the measured data from the 10° off-axis tensile specimen are within the range of the values reported elsewhere. The spread in the available data is due to variations in fiber volume ratio (0.45 to 0.70) and due to the test method used.

The previous comparisons lead to the conclusion that the 10° off-axis tensile specimen appears to be a good specimen for intralaminar shear characterization from both the theoretical and experimental viewpoints.

RECOMMENDATION

Based on the theoretical and experimental results of this investigation, it is recommended that the 10° off-axis tensile test specimen be considered as a possible standard test specimen for characterizing the intralaminar shear properties of unidirectional fiber composites.

A schematic depicting the geometry and instrumentation of the recommended test specimen is shown in Fig. 12. Note that it is advisable to use two back-to-back delta rosette strain gages to account for possible out-of-plane bending. The procedures previously described may be used for specimen preparation, instrumentation, mounting in the test fixture, and data acquisition and reduction. The ASTM D3039-74 test procedure may also be used as a guide.

The distinct advantages of the 10^{o} off-axis tensile specimen as a standard for intralaminar shear characterization compared to current practice are:

(1) Use of a familiar tensile test procedure (ASTM D3039-74)

(2) Use of thin laminate narrow specimens which save considerable material compared to thin tubes

(3) Test specimens may be cut from the same laminate as test specimens for longitudinal and transverse properties characterization

(4) Specimens have uniform shear stress through the thickness

(5) Specimens can be easily adapted to testing for environmental and elevated temperature effects

(6) Specimens can be readily used for crack propagation, fracture mechanics and fatigue testing

(7) Specimens are suitable for dynamic and impact loading characterization

(8) The test yields, in addition to intralaminar shear properties, the following off-axis properties: modulus, Poisson's ratio, coupling between extensional and shear deformations, and fracture stress

(9) Specimens are free of lamination residual stresses in contrast to the $\pm 45^{o}$ specimen

(10) The intralaminar shear strain reaches or approaches its maximum when the angle between load and fiber directions is about 10^{o}

(11) The specimen has been used successfully for high-strain-rate intralaminar shear characterization[8]

The disadvantages of the 10° off-axis tensile specimen are:

(1) Need to measure three strains at a point

(2) Need to transform both strains and stresses

(3) Care in test specimen preparation

(4) Care in alining strain gage on specimen and specimen in load fixture

(5) Need relatively long specimen gage-length to gage-width -14 or greater)

CONCLUSION

A combined theoretical and experimental investigation was performed to assess the applicability of the 10° off-axis tensile specimen for the intralaminar shear characterization of unidirectional fiber composites. The results of this investigation led to the recommendation that the 10° off-axis tensile specimen be considered as a possible standard test for intralaminar shear characterization of unidirectional fiber composites.

REFERENCES

1. Bert, C. W., "Experimental Characterization of Composites. Composite Materials," Vol. 8, Pt. 2, C. C. Chamis, ed., Academic Press, New York, 73-133 (1975).

2. Daniel, I. M. and Liber, T., "Lamination Residual Stresses in Fiber Composites," IIT Research Institute Report IITRI-D6073-1 (1975); also NASA CR-134826.

3. Chamis, C. C., "Failure Criteria for Filamentary Composites," NASA TN D-5367 (1969).

4. Chamis, C. C., "Failure Criteria for Filamentary Composites," STP 460. Composite Materials: Testing and Design, Am. Soc. for Testing and Materials, New Orleans, 336-351 (1972).

5. "Transverse Sensitivity Errors," Micro-Measurements, Technical Note 137.

6. Chamis, C. C., Kring, J. F., and Sullivan, T. L., "Automated Testing Data Reduction Computer Program," NASA TM X-68050 (1972).

7. Chamis, C. C. and Sullivan, T. L., "Combined-Load Stress-Strain Relationships of Fiber Composite Laminates," NASA TM X-71825 (1976).

8. Daniel, I. M. and Liber, T., "Strain Rate Effects on Mechanical Properties of Fiber Composites," IIT Research Institute Report IITRI-D6073-IV (1976); also NASA CR-135087.

TABLE I. - FRACTURE STRESSES AND COMPARISON WITH PLY STRENGTHS FOR MOD-I/EPOXY SPECIMENS

(a) Measured ply strengths

Load direction	Strength	
	N/cm^2	ksi
0° (longitudinal tensile $S_{\ell 11T}$)	56.3×10^3	81.7
90° (transverse tensile $S_{\ell 22T}$)	2.8	4.0
0° Tube (torsion $S_{\ell 12S}$)	5.2	7.6
10°	34.3	49.8

(b) Computed ply fracture stresses at the 10° plane

Stress type	Fracture stress	
	N/cm^2	ksi
Longitudinal $\sigma_{\ell 11}$ (along fibers)	33.3×10^3	48.3
Transverse to fibers $\sigma_{\ell 22}$	1.0	1.5
Intralaminar shear $\sigma_{\ell 12}$	5.9	8.5

(c) Comparison of ply fracture stresses at the 10° plane ply strengths

Stress type	Ply strength		Computed ply fracture stress at the 10° plane		Ratio of computed ply fracture stress to ply strength
	N/cm^2	ksi	N/cm^2	ksi	
Longitudinal	56.3×10^3	81.7	33.3×10^3	48.3	0.59
Transverse	2.8	4.0	1.0	1.5	.38
Intralaminar shear	5.2	7.6	5.9	8.5	1.12

TABLE II. - UNIDIRECTIONAL COMPOSITE PROPERTIES

Property	Composite		
	Mod-I/epoxy	T-300/epoxy	S-glass/epoxy
Longitudinal tensile modulus, $E_{\ell 11}$, N/cm^2 (psi)	24.1×10^6 (34.9×10^6)	13.2×10^6 (19.1×10^6)	4.72×10^6 (6.84×10^6)
Transverse tensile modulus, $E_{\ell 22}$, N/cm^2 (psi)	0.772×10^6 (1.12×10^6)	0.800×10^6 (1.16×10^6)	1.34×10^6 (1.94×10^6)
Shear modulus, $G_{\ell 12}$, N/cm^2 (psi)	0.610×10^6 (0.89×10^6)	0.434×10^6 (0.63×10^6)	0.648×10^6 (0.94×10^6)
Longitudinal Poisson's ratio, $\nu_{\ell 12}$	0.218	0.394	0.316
Longitudinal tensile fracture stress, $S_{\ell 11T}$, N/cm^2 (ksi)	56.3×10^3 (81.7)	128×10^3 (186)	129×10^3 (188)
Transverse tensile fracture stress, $S_{\ell 22T}$, N/cm^2 (ksi)	2.8×10^3 (4.0)	4.2×10^3 (6.2)	4.5×10^3 (6.5)

TABLE III. - COMPARISON OF MEASURED INTRALAMINAR SHEAR PROPERTIES FROM 10^o OFF-AXIS TENSILE SPECIMEN WITH THOSE REPORTED ELSEWHERE

Composite	10^o Off-axis tensile specimen		Reported elsewhere				10^o Off-axis tensile specimen		Reported elsewhere			
			Low		High				Low		High	
	Modulus						Fracture stress					
	N/cm^2	psi	N/cm^2	psi	N/cm^2	psi	N/cm^2	ksi	N/cm^2	ksi	N/cm^2	ksi
Mod-I/epoxy	0.61×10^6	0.88×10^6	0.44×10^6	0.64×10^6	0.62×10^6	0.90×10^6	5.9×10^3	8.6	4.7×10^3	6.8	6.1×10^3	8.9
T-300/epoxy	.43	.63	.42	.61	.69	1.00	8.3	12.1	6.2	9.0	9.2	13.3
S-glass/epoxy	.65	.94	.57	.83	1.2	1.74	7.1	10.3	4.5	6.5	12	17.1

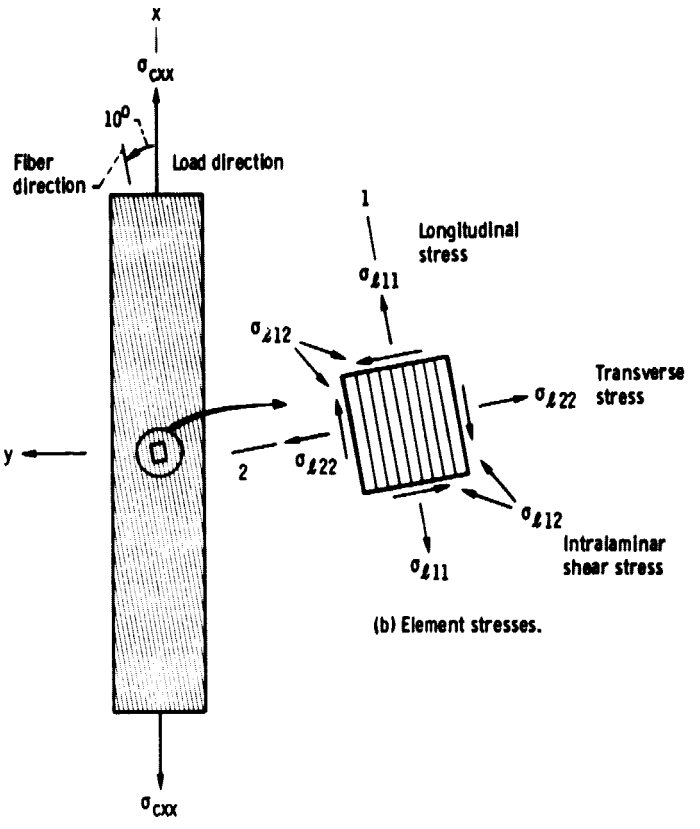

(b) Element stresses.

(a) Loaded specimen.

Figure 1. - Schematic depicting loaded 10^0 off-axis tensile test specimen and stresses at element at 10^0-plane (x, y - structural axes; 1, 2 - material axes).

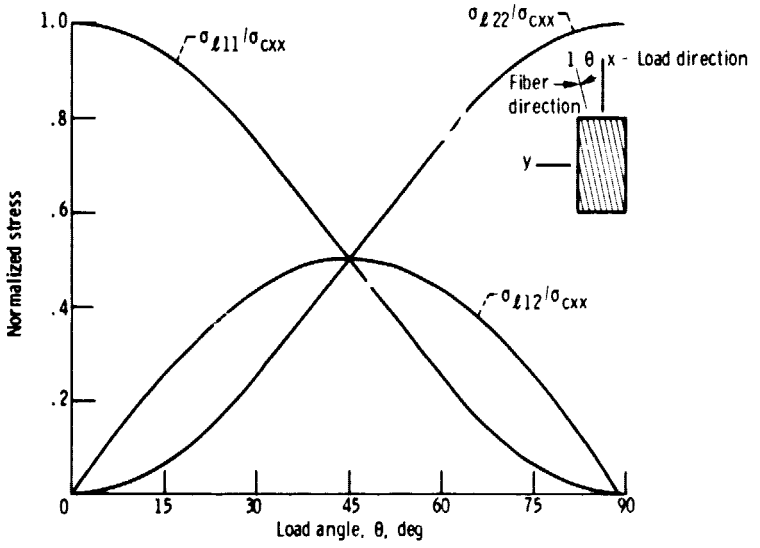

Figure 2. - Variation of material axes stress in unidirectional composite plotted against load direction.

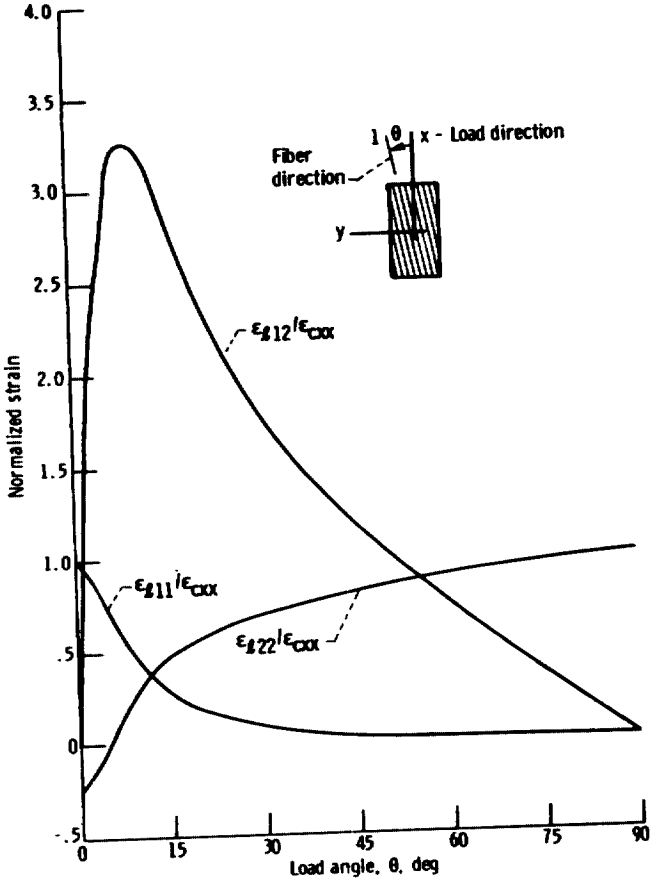

Figure 3. - Variation of material axes strains in unidirectional composite (Mod-I/epoxy) plotted against load direction.

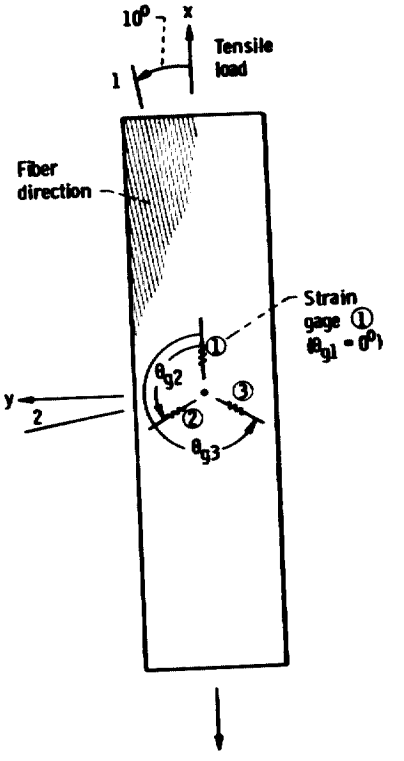

Figure 4. - Schematic depicting 10^0 off-axis tensile test specimen with strain gage positions (x, y - structural axes; 1, 2 - material axes).

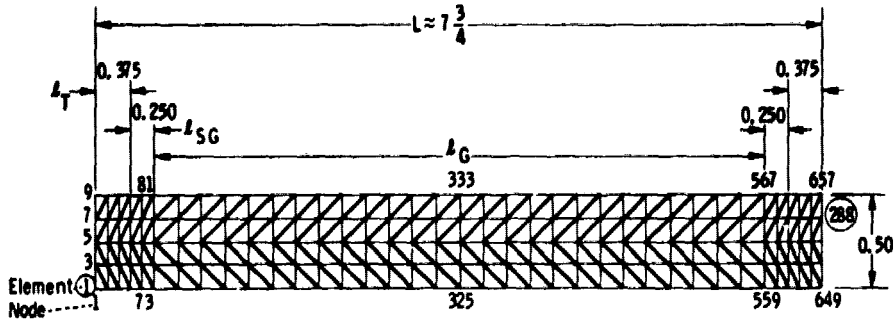

SYMBOLS:

L	length of test section ℓ_G plus tapered portion of end tabs
ℓ_T	length of tapered portion of Micarta end tabs
ℓ_{SG}	section just beyond tapered portion of end tabs and site of top gages

Figure 5. - Grid for finite element analysis of Mod-I/epoxy specimens. (Top gages located at nodes 74 and 77; midpoint gages located at nodes 326, 329, and 332. All dimensions shown are relative.)

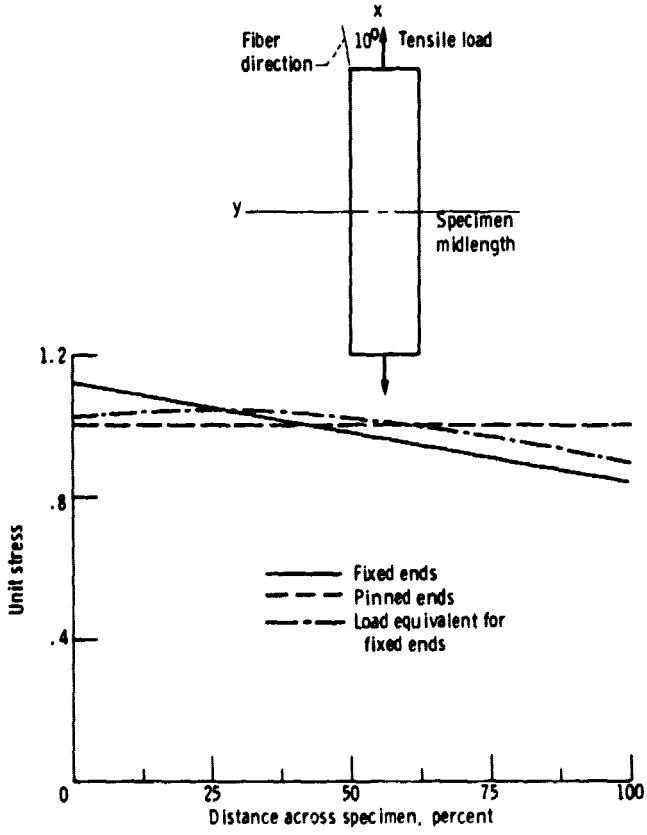

Figure 6. - Finite element analysis results of axial stress variation at midlength for three different boundary conditions; Mod-I/epoxy 10° off-axis tensile specimen. (See fig. 5 for finite element representation.)

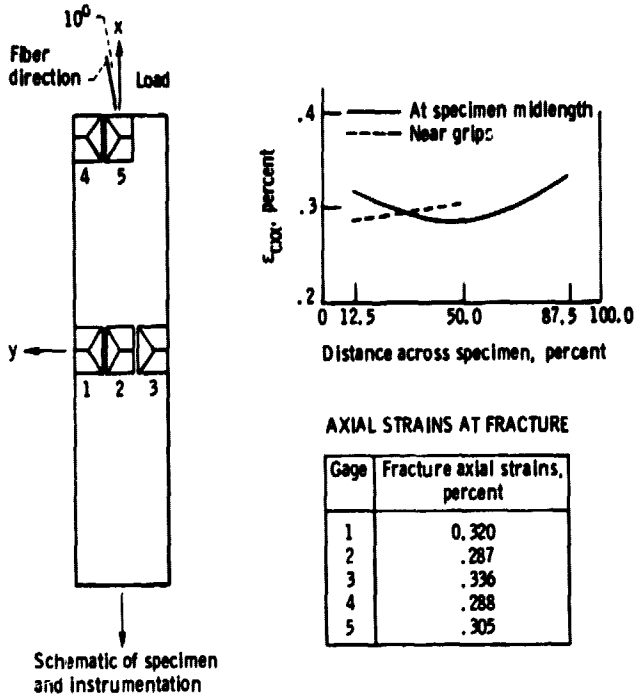

AXIAL STRAINS AT FRACTURE

Gage	Fracture axial strains, percent
1	0.320
2	.287
3	.336
4	.288
5	.305

Figure 7. - Axial strain variation across specimen of Mod-I/epoxy unidirectional composite $[0]_8$ loaded to fracture at 10° from fiber direction.

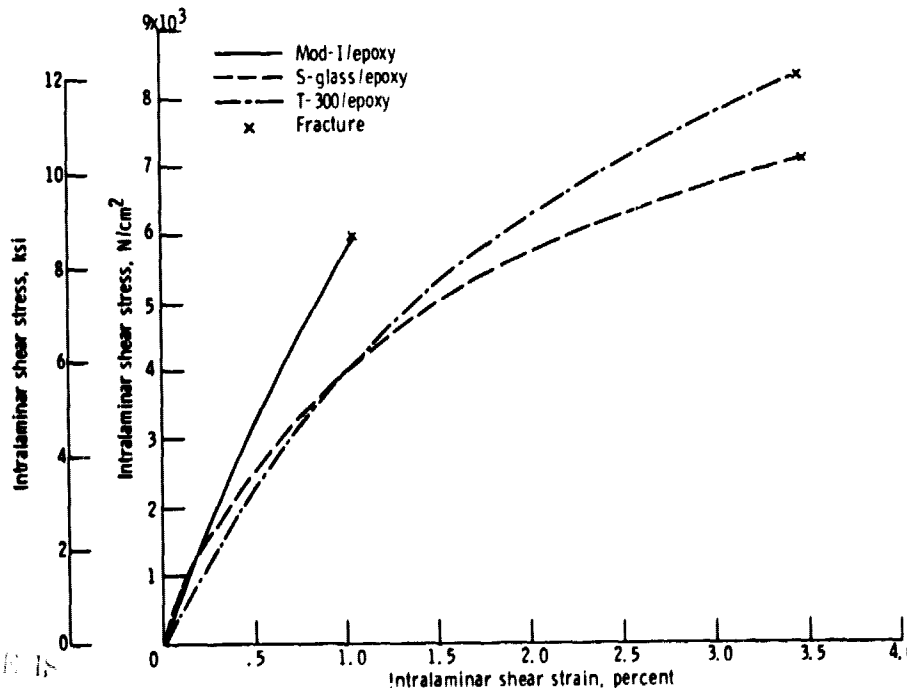

Figure 8. - Intralaminar shear stress-strain diagrams for three materials.

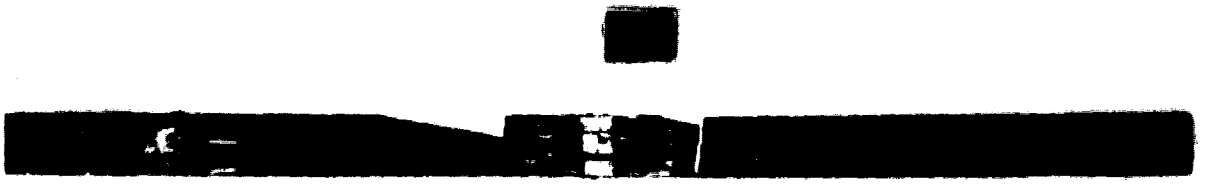

C-75-1177

(a) Front side.

C-75-1178

(b) Back side.

Figure 9. - Photograph of fractured 10° off-axis tensile specimen. Mod-I epoxy fiber composite.

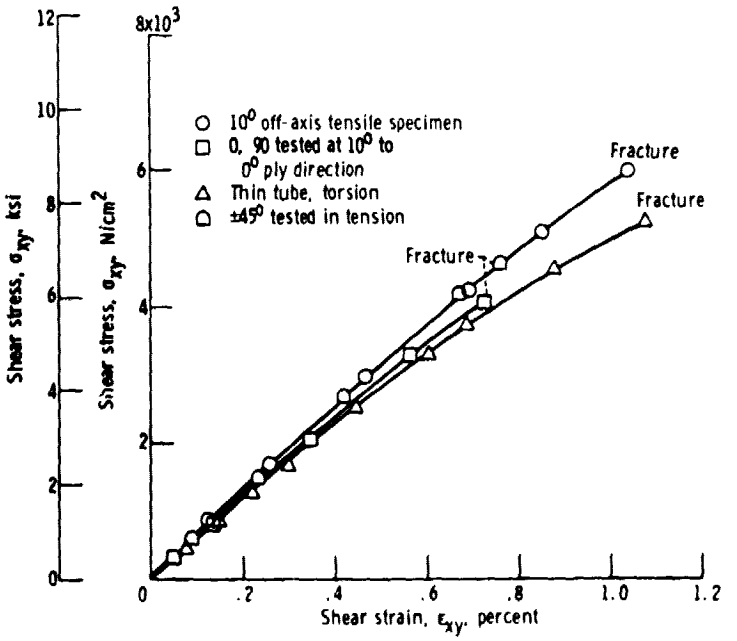

Figure 10. - Comparison of shear stress-strain curves.

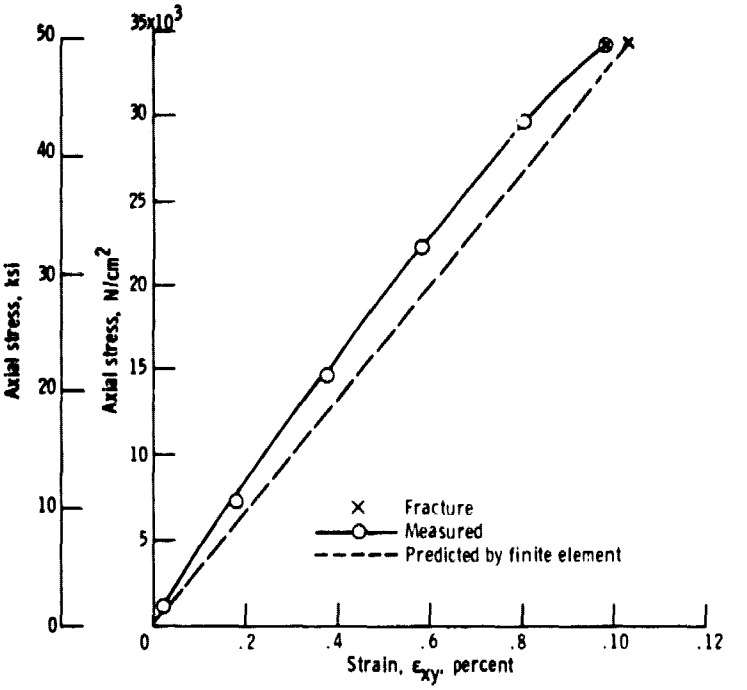

Figure 11. - Comparison of measured and predicted structural axes shear strains at center point of 10^0 off-axis tensile specimen (Mod I/epoxy fiber composite).

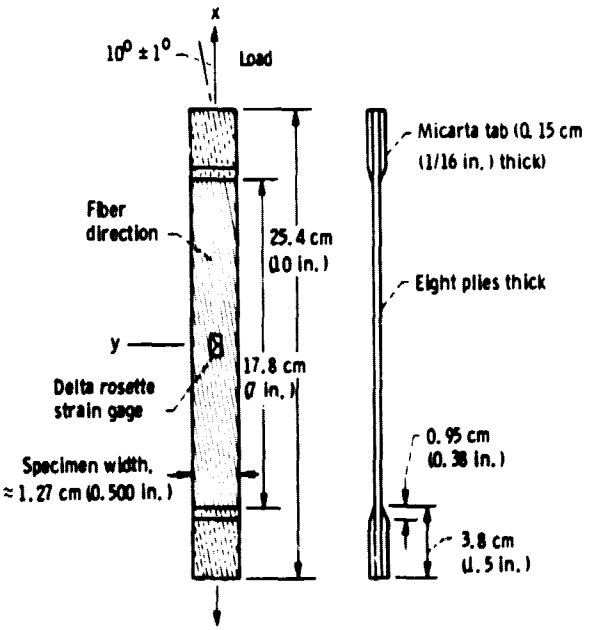

Figure 12. - Schematic showing geometry and instrumentation of proposed 10^0 off-axis tensile specimen for fiber composite intralaminar shear characterization.